Contribution of individual ionic currents to activity of a model stomatogastric ganglion neuron

Article *in* Journal of Neurophysiology · March 1992

DOI: 10.1152/jn.1992.67.2.341 · Source: PubMed

4 authors, including:

Jorge Golowasch
New Jersey Institute of Technology

Eve Marder
Brandeis University

Irving R Epstein
Brandeis University

JOURNAL OF NEUROPHYSIOLOGY
Vol. 67, No. 2, February 1992. Printed in U.S.A.

Contribution of Individual Ionic Currents to Activity of a Model Stomatogastric Ganglion Neuron

JORGE GOLOWASCH, FRANK BUCHHOLTZ, IRVING R. EPSTEIN, AND EVE MARDER
Departments of Biology and Chemistry, and Center for Complex Systems, Brandeis University, Waltham, Massachusetts 02254-9110

SUMMARY AND CONCLUSIONS

1. The behavior of the mathematical model for the lateral pyloric (LP) neuron of the crustacean stomatogastric ganglion (STG) developed in the previous paper was further studied.

2. The action of proctolin, a neuromodulatory peptide that acts directly on the LP neuron, was modeled. The effect of the proctolin-activated current (i_{proc}) on the model neuron mimics the effects of proctolin on the isolated biological LP neuron. The depolarization and increased frequency of firing seen when i_{proc} is activated are associated with changes in the relative contributions of the delayed rectifier (i_d) and the Ca^{2+}-activated outward current ($i_{o(Ca)}$) to the repolarization phase of the action potential.

3. The effects of turning off the A-current (i_A) in the model were compared with those obtained by pharmacologically blocking i_A in the biological neuron. i_A appears to regulate action-potential frequency as well as postinhibitory rebound activity.

4. The role of i_A on the rhythmic activity of the cell was studied by modifying several of its parameters while periodically activating a simulated synaptically activated conductance, i_{syn}.

5. The effects of manipulations of the maximal conductances ($\bar{g}$) for i_d and $i_{o(Ca)}$ were studied. i_d strongly influences action-potential frequency, whereas $i_{o(Ca)}$ strongly influences action-potential duration.

6. Modifications of the maximal conductance of the inward Ca^{2+} current (i_{Ca}) were compared with the effects of blocking i_{Ca} in the real cell.

7. The role of the hyperpolarization-activated inward current (i_h) during ongoing rhythmic activity was assessed by periodically activating i_{syn} while modifying i_h.

INTRODUCTION

One of the major motivations behind the construction of conductance-based neuronal models is to obtain and develop insights into the role that specific conductances play in controlling the excitability and firing properties of a neuron. Because models, unlike living cells, give the investigator direct access to information concerning all the currents simultaneously as the membrane potential varies with time, they allow us to see directly the relative values of multiple currents in a way not possible with electrophysiological recordings. In this paper we study the model developed in the previous paper (Buchholtz et al. 1992) by perturbing it in different ways: current injection, modifying parameters, and turning currents on or off. On the one hand, we use these perturbations to compare the model's behavior with that shown by the real neuron. On the other hand, we use the perturbed model to understand better the role that the major time- and voltage-dependent conductances play in shaping the behavior of the lateral pyloric (LP) neuron.

METHODS

The model employed in these studies is that developed in the preceding paper (Buchholtz et al. 1992). We shall refer to the model with the parameters in Table 1 of that paper as the standard model. The behavior of the cell is governed by the equation

$$c_m \cdot dV/dt = i_{ext} - \sum_j i_j \quad (1)$$

where c_m is the membrane capacitance of the cell, V is the membrane potential, i_{ext} is the applied current, and $\sum_j i_j$ is the sum over the seven currents described by Buchholtz et al. (1992), plus the two additional currents described below.

Current-clamp experiments are simulated simply by fixing i_{ext} at the appropriate value. Application of tetrodotoxin (TTX) is simulated by turning off the sodium current, i_{Na} (i.e., $\bar{g}_{Na} = 0\ \mu S$); application of 4-aminopyridine (4-AP) is simulated by turning off the A-current, i_A (i.e., $\bar{g}_A = 0\ \mu S$). In addition to the currents previously described, two other currents were added to the model for this paper. The first, the proctolin-activated current, i_{proc}, is described in the RESULTS. However, in some experiments, i_{proc} was turned on in such a way as to mimic a transient pressure application of proctolin. The diffusion of a square pulse of pressure-applied proctolin solution was simulated by making the maximal proctolin conductance $\bar{g}_p$ proportional to the difference of two exponential functions, one representing the input pulse, the other the removal of the peptide

$$\bar{g}_p = (0.1\ \mu S) \cdot f \quad (2)$$

where the proctolin activation function f is given by

$$f = 1.25[e^{-0.4(t)} - e^{-2.0(t)}] \quad (3)$$

and t is the time in seconds.

A second added current (i_{syn}) was used in some experiments to simulate inhibitory postsynaptic potentials (IPSPs) that the LP neuron routinely receives. Consistent with the treatment of Getting (1989), postsynaptic potentials were modeled with

$$i_{syn} = \bar{g}_{syn} \cdot a_{syn}(t) \cdot (V - E_K) \quad (4)$$

$$a_{syn}(t) = \sum_j a_j(t) \quad (5)$$

$$da_j/dt = \exp(-k_1 \cdot [t - j\Delta t]) - k_2 \cdot a_j \quad (6)$$

where $\bar{g}_{syn} = 0.15\ \mu S$, $E_K = -80$ mV, $k_1 = 50\ s^{-1}$, $k_2 = 20\ s^{-1}$, and $\Delta t = 20$ ms. *Equation 5* describes the temporal summation of each synaptic potential a_j, and j runs from 0 to 10 in our case. Figure 1 illustrates the time course and amplitude changes of the activation parameter a_{syn} (*Eq. 5*) during a simulated burst of synaptic potentials, showing the temporal summation and the slow time course of the envelope that characterizes the IPSPs that the real LP neuron receives (Eisen and Marder 1982; Hartline and Gassie 1979; Marder 1984; Fig. 2*A* in Golowasch and Marder 1992a).

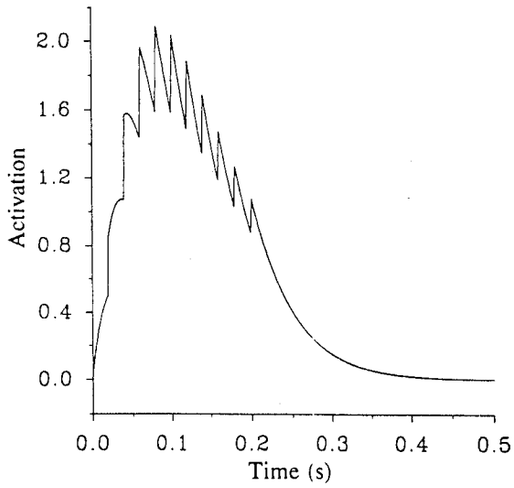

FIG. 1. Synaptic current activation. $a_{syn}(t)$ (*Eqs. 5* and *6*) during 1 burst of simulated presynaptic activity. Activation values higher than 1 are obtained because of temporal summation that occurs at the presynaptic frequency used.

Physiological experiments on LP neurons shown in this paper were carried out as described in Golowasch and Marder (1992a).

RESULTS

Biophysical analysis

One of the most instructive aspects of a model of this type is the ability one gains to dissociate the cell's activity pattern into its component parts, current by current. Figure 2 shows the activity of the model cell with all the currents of the standard model (Buchholtz et al. 1992) maximally activated. The *top panel* corresponds to the membrane potential and shows the tonic firing of overshooting action potentials, the form of which resembles that of those recorded from the cell body of the LP cell (Fig. 5 in Buchholtz et al. 1992), except that in the real cell they are attenuated by the filtering imposed by the cable formed by the neurite's membrane between the spike initiation zone and the soma. A frequency of 8.5 Hz and a baseline of −48 mV are observed.

The *middle five panels* of Fig. 2 show the contribution of the currents that are playing a role during tonic activity (i_h is not shown because at these membrane potentials it is virtually inactive). The largest current is i_{Na}, which dominates both the initiation and the termination of the action potentials. As in the Hodgkin and Huxley (1952) model, it is the inactivation of i_{Na} that initiates the termination of the action potential. The shoulder in the Na^+ current trace is the result of the very fast change in driving force as V rapidly approaches E_{Na}. Because the inactivation of this current is slow compared with its activation, as the outward currents begin activating, thus forcing the cell to hyperpolarize, the driving force increases again before the current completely inactivates, giving rise to the secondary increase of inward current.

During tonic activity (Fig. 2) the Ca^{2+}-activated outward current, $i_{o(Ca)}$, turns on faster than the delayed rectifier, i_d, so that $i_{o(Ca)}$ contributes at least as much outward current as i_d to action-potential termination (see below). In the first phase, $i_{o(Ca)}$ is the dominant current, whereas i_d dominates most of the second phase of the action-potential repolarization (Fig. 2, *3rd and 4th panels*). Under these conditions, i_A turns on rather slowly and is quite small, and provides only a minor contribution to the waveform of the action potential, although it does influence firing frequency (see below). i_{Ca} contributes a small inward current to the pacemaker potential and the intracellular Ca^{2+} concentration [Ca] increase (Fig. 2, *bottom panel*) necessary to activate $i_{o(Ca)}$, which in turn is the primary source of outward current for the early repolarizing phase. Finally, the leak current, i_l, (not shown) passively and instantaneously follows the voltage changes and thus is a perfect reflection of V.

Proctolin-activated current, i_{proc}

Proctolin is a neuropeptide found in identified inputs to the stomatogastric ganglion (STG) (Nusbaum and Marder

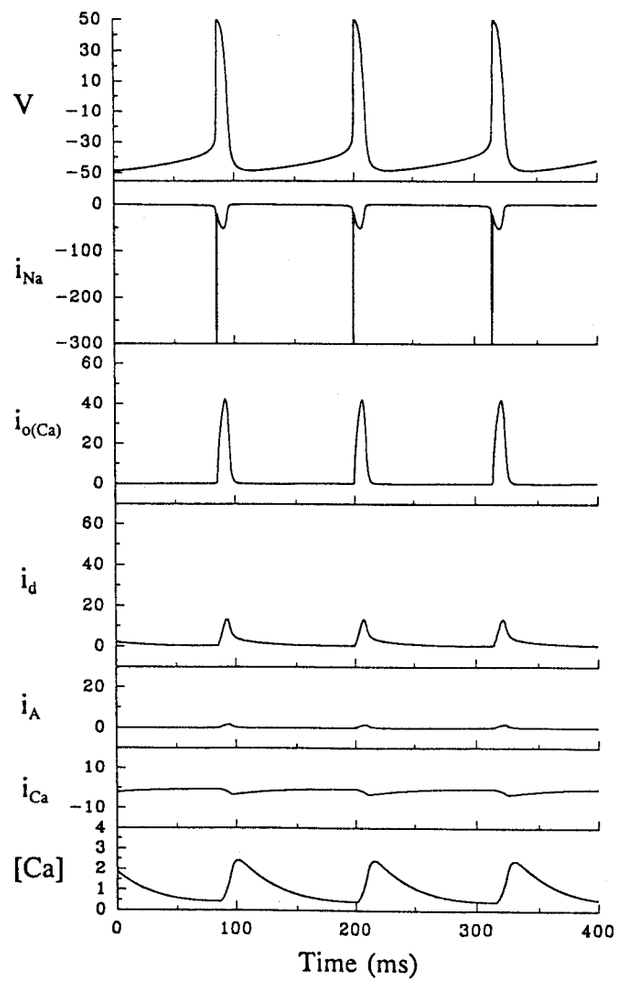

FIG. 2. Activity of the model cell and contributing conductances. Integration of *Eq. 1* of the standard model (Table 1 of Buchholtz et al. 1992). i_{ext} = 0 nA. V (*top panel*) is in millivolts, current amplitudes (*middle panels*) are in nanoamperes, and Ca^{2+} concentration (*bottom panel*) is in micromolar.

1989a,b). The LP neuron is a direct target for proctolin and responds to proctolin application with a small depolarization and increase in firing frequency (Marder et al. 1986; Hooper and Marder 1987; Nusbaum and Marder 1989a,b; Golowasch and Marder 1992b). Golowasch and Marder (1992b) characterized the voltage and time dependence of the current evoked by proctolin in the LP neuron and found that i_{proc} is maximal at values close to the resting potential, and that the current activates very rapidly without apparent voltage-dependent inactivation. We have thus defined i_{proc} as governed by a single activation process p, the dynamics of which are given by the standard *Eqs. 1–3* of Buchholtz et al. (1992) with a voltage-independent k_p. The parameters we used are as follows: maximal conductance $\bar{g}_p = 0.09\ \mu S$, reversal potential $E_p = -10$ mV, rate constant $k_p = 166\ s^{-1}$, half-maximal potential $V_p = -55$ mV, and step width $s_p = -5$ mV [see METHODS (*Eqs. 1–3*) in Buchholtz et al. 1992].

In Fig. 3 we show the calculated i_{proc} (Fig. 3*A*), illustrating the kinetics of the activation process, and the steady-state activation $p_\infty(V)$ (Fig. 3*B*). Because E_p is −10 mV, the decreased driving force as the voltage increases toward E_p (where the current is fully activated) yields the inverted bell-shaped appearance that has been measured in the LP cell (Golowasch and Marder 1992b). Note that its amplitude is markedly voltage dependent (Fig. 3*A*), it activates within several milliseconds, and does not inactivate (unless proctolin is removed).

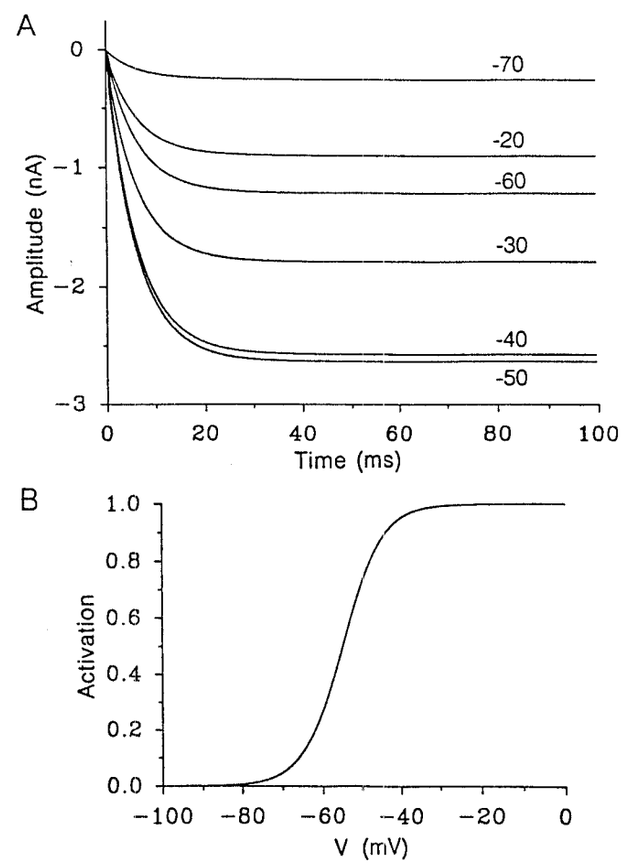

FIG. 3. Model proctolin-activated current. *A*: time course of the calculated i_{proc} for different voltages (indicated above the traces except for −50). *B*: steady-state activation $p_\infty(V)$ shown as a function of membrane potential.

Simulation of pharmacological manipulations

Figure 4 compares the effect of a simulated transient pressure application of proctolin on the model neuron with the response of the real cell. Note that both the model (Fig. 4*A*) and the real neuron (Fig. 4*B*) depolarize slowly by several millivolts and start firing action potentials at a higher rate.

Figure 5 allows us to look at the individual currents and their relationship during steady activation of i_{proc}. With i_{proc} added to our standard model (Buchholtz et al. 1992), the model cell fires action potentials tonically at a frequency 19 Hz higher than control. The action potentials are slightly smaller in amplitude and ride on top of a baseline depolarized by 6 mV with respect to control (Fig. 5, Table 1). In addition to the frequency increase, the action-potential duration increases by ~10% (Table 1). Furthermore, incorporation of i_{proc} into the standard model has a surprising consequence: the relative contributions of $i_{o(Ca)}$ and i_d change, the former becoming smaller and the latter becoming larger (compare *the 3rd and 4th panels* between Figs. 2 and 5). The drop in $i_{o(Ca)}$ is unexpected because with proctolin the level of intracellular [Ca] is always higher, which should tend to increase the activation of $i_{o(Ca)}$. However, the Ca^{2+} dependence of the inactivation of $i_{o(Ca)}$, which causes the conductance to decrease for high [Ca] (see Fig. 2*B* of Buchholtz et al. 1992), apparently overcomes this tendency.

Simulating the effects of TTX by inactivating i_{Na} in the model completely eliminates the action potentials (not shown) and leaves the cell at a resting potential of −49 mV, which compares well with the average experimental resting potential V_{rest} of −48.9 mV (Golowasch and Marder 1992a).

i_A has relatively minor effects on the activity of the model cell when it is unperturbed by inputs. However, a small effect on the firing frequency might be expected from the results shown in Fig. 2 (*5th panel*). In fact, turning off i_A increases the frequency by ~14%, but with only minimal effects on the action-potential duration or the membrane potential baseline (Table 1). This effect on the firing frequency, which was sometimes observed in LP cells bathed in 4-AP to block i_A, is consistent with Fig. 3*B* of Buchholtz et al. (1992), which indicates that some level of i_A activation exists at these voltages. i_A has a much more significant action after the LP neuron is hyperpolarized, as shown in Fig. 6. The complicated voltage dependence of i_A suggests that, after a hyperpolarizing current pulse, the firing frequency should transiently decrease and action-potential firing should be delayed by the strong transient activation of i_A. A 1-s prepulse to about −70 mV causes the model cell to delay the firing of its first action potential by ~100 ms and subsequently to show a firing frequency ~25% slower (Fig. 6*A*, *top*) than at steady state (Fig. 2, *top*). When i_A is turned off, this delay is shortened significantly, and the firing frequency quickly adjusts to its steady-state value of near 8.5 Hz (Fig. 6*A*, *bottom*). This behavior was confirmed in the

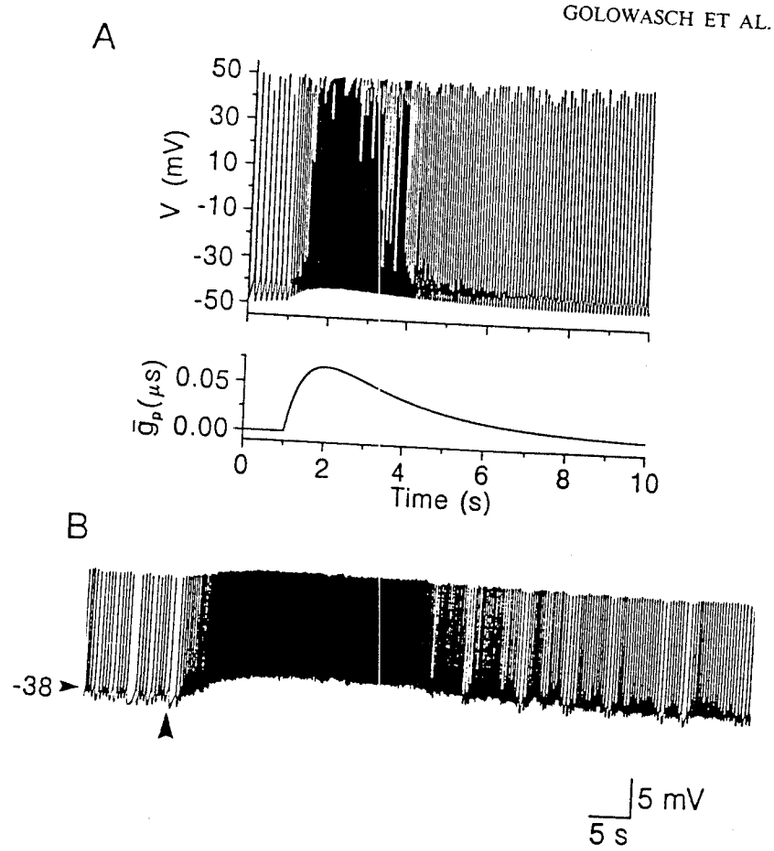

FIG. 4. Effect of a transient application of proctolin on the cell. *A*: model cell simulation. Standard model plus i_{proc}. $\bar{g}_p$ follows the time-dependent changes shown in the *bottom trace* (*Eqs. 2–4*). *B*: LP cell's experimental response to proctolin. The stomatogastric nerve (stn) is blocked. Measured in 10 μM PTX. Arrowhead indicates pressure application of 100 μM proctolin (0.5 s).

real LP cell with a similar current injection protocol (Fig. 6*B*) in control saline (*top*) and in the presence of 10 mM 4-AP (*bottom*), which blocks i_A (Golowasch and Marder 1992a).

Perturbing the maximum conductances of the outward currents has characteristic effects. Figure 7 shows the effect of changes in the maximum conductance of i_d (Table 1). When i_d is turned off ($\bar{g}_d = 0$ μS), the model cell depolarizes to approximately +5 mV, and action potentials are abolished. Decreasing $\bar{g}_d$ by a factor of 2 ($\bar{g}_d = 0.17$ μS) causes the baseline to depolarize by 15 mV, simultaneously increasing the firing frequency about threefold. Doubling $\bar{g}_d$ has the opposite effect, hyperpolarizing the baseline by 9 mV and decreasing the firing frequency to ~50% of the control level (Table 1). Modifications of i_d produced comparatively small changes on action-potential duration: a 20% increase was seen when $\bar{g}_d$ was decreased, and a 12% decrease was seen when $\bar{g}_d$ was increased twofold (Table 1). Taken together, these effects indicate that i_d has a stronger effect on the slow repolarization of the cell that contributes to firing frequency than on the spike termination.

Figure 8 shows the effect of $i_{o(Ca)}$ on the activity of the model cell. When $i_{o(Ca)}$ is completely inactivated ($\bar{g}_{o(Ca)} = 0$ μS), the cell's baseline depolarizes to approximately +5 mV, and the cell stops firing action potentials, as in the case of blocking i_d. If $\bar{g}_{o(Ca)}$ is decreased twofold ($\bar{g}_{o(Ca)} = 1.6$ μS), the baseline remains at control levels, and the firing frequency increases only ~2%. When $\bar{g}_{o(Ca)}$ is doubled ($\bar{g}_{o(Ca)} = 6.4$ μS), the baseline hyperpolarizes by 4 mV, and the firing frequency changes also by only ~2%. However, the same conductance changes evoke a 17% increase and a 14% decrease, respectively, in action-potential duration (Table 1). These observations suggest that $i_{o(Ca)}$ contributes mainly to the narrowing (termination) of the action potential and to a lesser extent to the repolarization governing firing frequency of the cell than i_d (compare Figs. 7 and 8, Table 1).

Blocking i_{Ca} causes a decrease in the frequency of tonic firing from 8.5 to 2.7 Hz, a broadening of the action potentials by ~46%, and a hyperpolarization of the baseline voltage by 13 mV (Fig. 9*A*, Table 1). The explanation of these effects can be found in Fig. 2, which shows that i_{Ca} contributes a small inward current to the cell that, if blocked, would cause the cell to hyperpolarize. It also contributes the necessary Ca^{2+} to activate $i_{o(Ca)}$. The broadening of the action potentials is the consequence of inactivating $i_{o(Ca)}$ and is consistent with the effects recorded in the LP cell. Figure 9*B* shows the effect of Cd^{2+} (which blocks both components of Ca in the real cell) on the firing activity of an isolated LP cell. Bath application of 200 μM Cd^{2+} hyperpolarizes the baseline, increases the duration of the action potentials, and increases slightly the action-potential amplitude, effects that are consistent with a blocking effect on i_{Ca} and $i_{o(Ca)}$. However, almost no effect on the action-potential frequency was observed (see DISCUSSION).

Because i_h activates at more hyperpolarized voltages than those the cell normally undergoes when isolated from chemical synapses, we have simulated IPSPs similar to those the

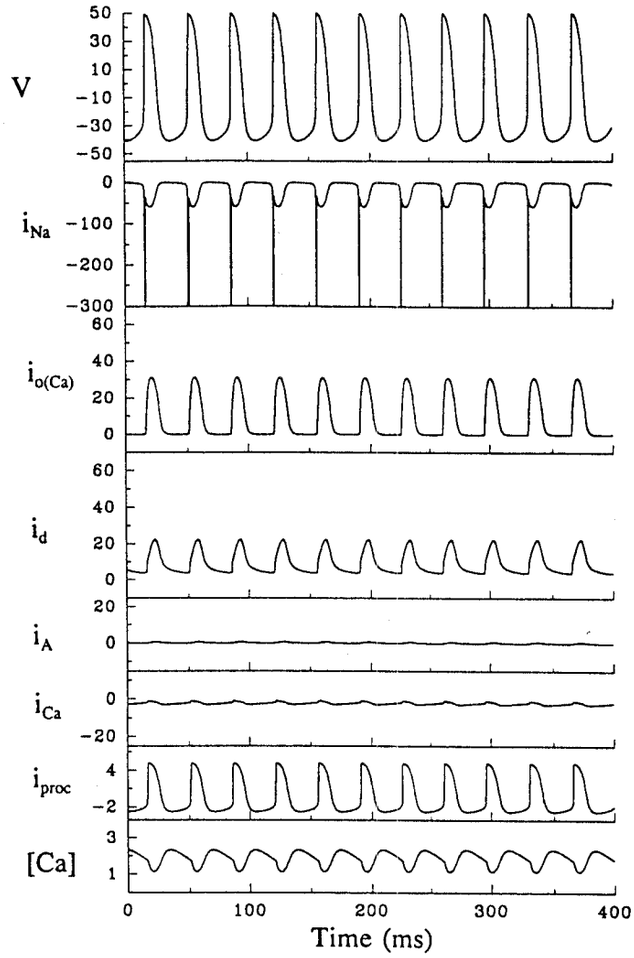

FIG. 5. Activity of the model cell and contributing conductances during activation of i_{proc}. Integration of *Eq. 1* of the standard model plus i_{proc} (described in the text). *V* (*top panel*) is in millivolts, current amplitudes (*middle panels*) are in nanoamperes, and [Ca] (*bottom panel*) is in micromolar. Notice the different relative amplitudes of $i_{o(Ca)}$ and i_d compared with Fig. 2.

LP cell receives from its synaptic neighbors (Eisen and Marder 1982; Hartline and Gassie 1979; Marder 1984; Fig. 2 in Golowasch and Marder 1992a) according to *Eqs. 4–6*. In Fig. 10, trains of 10 IPSPs 20 ms apart were applied at intervals of 1 s, and the effects of modifying i_h are illustrated. Inactivating i_h has no noticeable effect on the tonic firing of the model cell (not shown). Doubling $\bar{g}_h$ has a minor effect on the frequency of firing (compare *the 1st and 3rd traces* of Fig. 10). Additionally, doubling $\bar{g}_h$ has a small but clear effect on the phase at which a new burst of action potentials begin after a train of IPSPs. A shift of +15 mV in the activation curve of i_h (i.e., V_r = −55 mV instead of −70 mV) induces a much more pronounced effect both on the firing frequency and on the phase at which a new burst begins after a train of IPSPs (Fig. 10, *2nd panel*). A much stronger effect is observed when both of these changes are made simultaneously (Fig. 10, *4th panel*). Here a 70% increase in firing frequency and a 50% phase advance are observed. In addition to this, during the hyperpolarizing phase, the stronger i_h (Fig. 10, *bottom trace*) becomes activated enough to allow the cell to remain more depolarized throughout the inhibitory phase than in control conditions (Fig. 10, *top trace*). This effect would be expected to have a pronounced consequence on graded synaptic transmitter release (Graubard et al. 1983).

TABLE 1. *Effects of conductance modification on the model cell*

Condition*	Spike Duration, ms†	Firing Frequency, Hz	Baseline, mV
Control ($i_{proc\ OFF}$)	12.0	8.5	−48
$\bar{g}_p$ = 0.09 μS	13.2	27.5	−42
$\bar{g}_A$ = 0 μS	11.6	9.3	−48
$\bar{g}_d$ = 0.17 μS (½ control)	14.4	29.0	−33
$\bar{g}_d$ = 0.7 μS (2× control)	10.6	4.4	−57
$\bar{g}_{o(Ca)}$ = 1.6 μS (½ control)	14.0	8.7	−48
$\bar{g}_{o(Ca)}$ = 6.4 μS (2× control)	10.3	8.3	−52
$\bar{g}_{Ca}$ = 0 μS	17.5	2.7	−61

* $\bar{g}_p$ = 0 μS unless indicated.
† Measured at −20 mV.

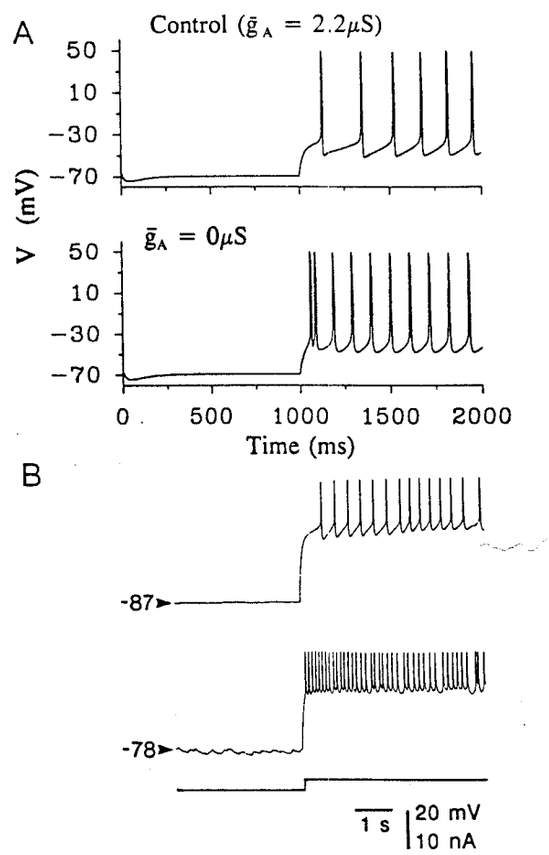

FIG. 6. Effect of i_A on the rebound activity of the cell. *A*: effect on model cell. Standard model; i_{proc} is turned off. At t = 0 ms, a pulse of i_{ext} = −3 nA is applied for 1,000 ms. *Top*: the control with i_A intact. *Bottom*: the same protocol but with $\bar{g}_A$ = 0 μS. *B*: effect on LP cell. Preparations in PTX, with the input nerve stn blocked. The cell was hyperpolarized by −3 nA for 15 s before releasing the current. Control is shown in the *top trace*, and the *bottom trace* shows the effect after a fast and short perfusion in 10 mM 4-AP (to minimize its toxic effects).

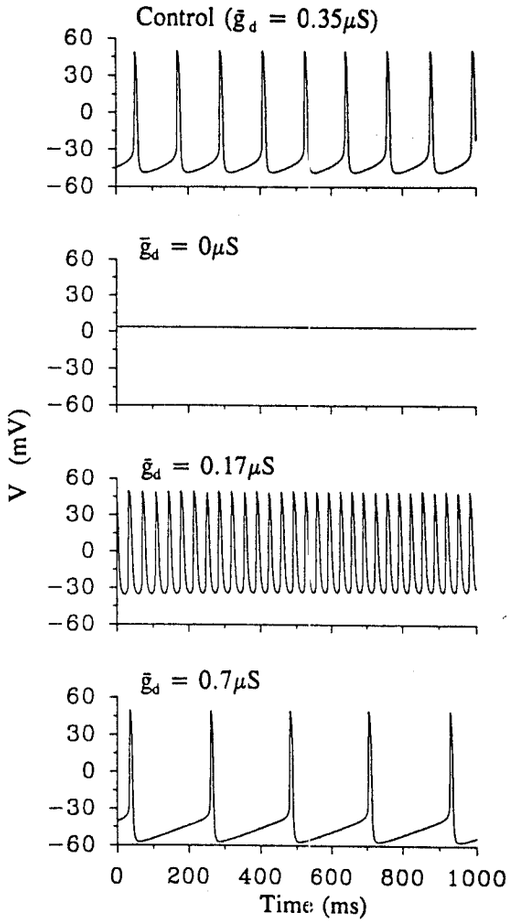

FIG. 7. Effect of modifying i_d on the activity of the model cell. Standard model with i_{proc} turned off. $\bar{g}_d$ values for each condition are indicated on the *top left corner* of each panel. Notice the marked effect on firing frequency and baseline voltage.

The latency from the end of the train of IPSPs to the first action potential is critical for timing in the pyloric rhythm. Hartline and Gassie (1979) have suggested that neurons that recover from synaptic inhibition more slowly may have a larger i_A, or they could have an i_A with shifted activation and inactivation curves. Figure 6 shows that i_A has a strong influence on the latency to the first spike after a hyperpolarization. Figure 11 shows the effect of modifying the voltage threshold (i.e., half-maximal potential) (see Buchholtz et al. 1992) for the inactivation (V_B) and the activation (V_A) processes of i_A in the postsynaptic cell. These parameters are expected to have the strongest effect in determining whether and in what voltage range i_A will turn on during the activity of the cell. If V_A is maintained at the control value of −12 mV, variations in the value of V_B from its standard value of −62 mV to values more positive than approximately −40 mV only have any effects on the cell's rebound from a simulated IPSP. At V_B = −40 mV (Fig. 11, *middle*), there is a small increase in the latency to the first action potential and a decrease in firing frequency. If V_B is kept constant at the value set for the standard version of the model, and V_A is lowered by ~30 mV, a dramatic increase in the delay of the postinhibitory firing occurs (Fig. 11, *bottom*), accompanied by a decrease in firing frequency. More negative values of V_A have even stronger effects, eventually abolishing spiking activity completely.

DISCUSSION

One of the difficult problems in neurobiology is understanding how each of the conductances present in a neuron shapes that neuron's electrical properties. In this paper we demonstrate that the role of several conductances changes when the cell moves from one voltage range to another, as is the case when i_{proc} is included in our standard model. Although this result is not unexpected, there is no obvious a priori way to predict, from voltage-clamp experiments on isolated currents alone, what each current will contribute to the dynamic pattern of activity of the neuron.

Proctolin is found in identified modulatory inputs to the STG (Nusbaum and Marder 1989a,b). The stimulation of the proctolin-containing neurons, or the exogenous appli-

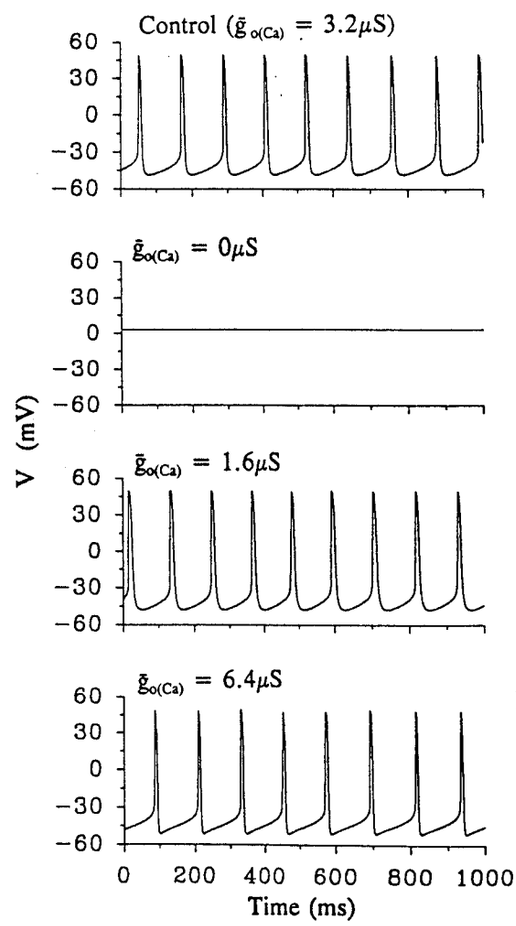

FIG. 8. Effect of modifying $i_{o(Ca)}$ on the activity of the model cell. Standard model with i_{proc} turned off. $\bar{g}_{o(Ca)}$ values for each condition are indicated on the *top left corner* of each panel. Notice the effect on action-potential duration and the lack of effect on firing frequency.

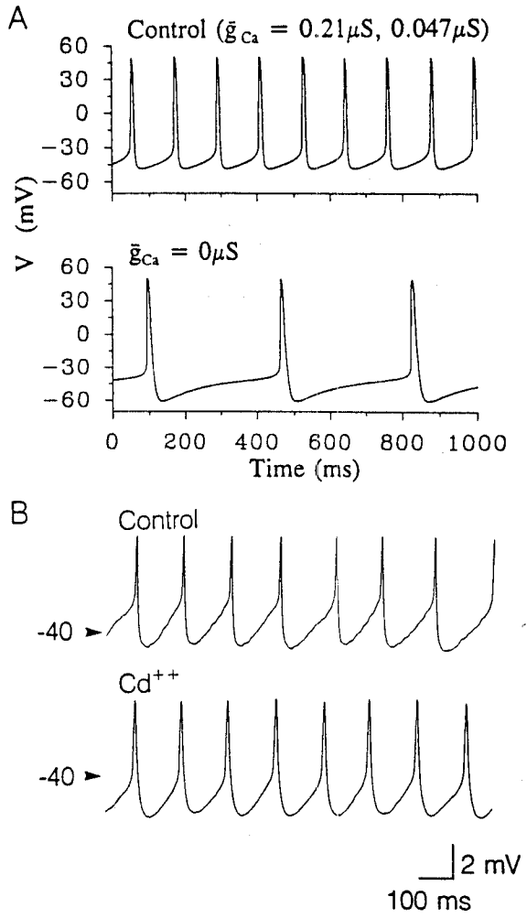

FIG. 9. Effect of blocking i_{Ca}. *A*: standard model with i_{proc} turned off. *Top*: control. *Bottom*: $\bar{g}_{Ca}$ set to 0 μS for both components (see Table 1 in Buchholtz et al. 1992). *B*: effect of Cd^{2+} on the firing activity of the experimental LP cell. LP in PTX and stn input nerve blocked. *Top*: control. *Bottom*: in 200 μM bath-applied Cd^{2+}.

cation of proctolin, strongly excites the LP neuron (Hooper and Marder 1987; Marder et al. 1986; Nusbaum and Marder 1989a,b) (Fig. 4). Golowasch and Marder (1992b) studied the proctolin-evoked current in LP neurons and found that proctolin activates a small inward current that is markedly voltage dependent, and largest at membrane potentials close to the LP neuron's baseline membrane potential and threshold for action-potential activation. However, it was quite puzzling that a small current could produce such a dramatic increase in the frequency of the LP neuron firing. Our ability to examine individually the currents in the LP neuron with the use of the model allows us to offer an explanation for this effect. In the absence of proctolin, $i_{o(Ca)}$ is the predominant outward current that terminates the action potential (Fig. 2). In the presence of proctolin, $i_{o(Ca)}$ is diminished, resulting in an action potential slightly longer in duration [Fig. 5; at −20 mV the duration of the action potential is 12.0 ms in control conditions (Fig. 2, Table 1) and 13.2 ms in proctolin (Fig. 5, Table 1)]. Because i_d plays an important role in controlling the frequency of firing (Fig. 8), it is interesting that in the presence of proctolin the frequency increases despite the substantial increase in i_d. Presumably this occurs because the frequency that would be expected by the augmentation of i_d is overpowered by the changes in the other currents that control the frequency. Therefore it is informative to use the plots in Figs. 2 and 5 to obtain at least a qualitative understanding of the factors that control the firing rate of the LP neuron in the absence (Fig. 2) and the presence of proctolin (Fig. 5). In the absence of proctolin the interspike interval is influenced by three factors: *1*) the turning off of i_d, *2*) the inactivation of i_{Ca}, and *3*) the recovery from inactivation of i_{Na}. i_d and i_{Ca} turn off in such a way that these two effects almost balance. However, although it is not evident at the scale shown in Fig. 2, an appreciable i_{Na} develops during the interspike interval, which plays an important role in bringing the cell to threshold. Proctolin adds a modest noninactivating inward current at all hyperpolarized membrane potentials. Note also, in proctolin, that there is a small permanent net inward i_{Ca} throughout the voltage range. This results in a shift of the baseline membrane potential by ~10 mV. Once again, the interspike interval is determined by the interactions among i_{Na}, i_{Ca}, and i_d, and it is diminished because the threshold, which remains constant in proctolin, is reached sooner from the depolarized baseline.

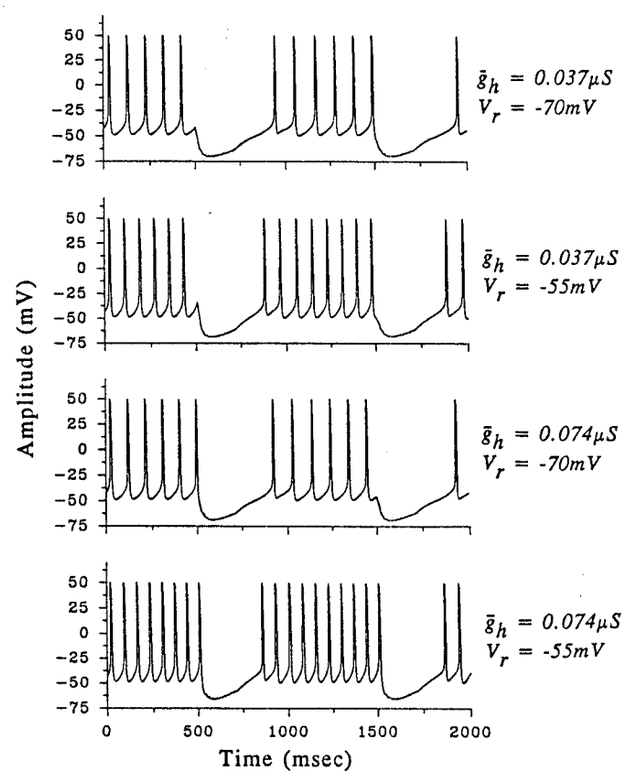

FIG. 10. Model cell's synaptic potentials: effect of i_h. Parameters as listed in Table 1 of Buchholtz et al. (1992). Presynaptic activity is bursts of 10 IPSPs at 50 Hz every 1 s. *Top*: control. Parameter modifications are indicated to the *right* of each trace. Notice the dramatic effect on the phase at which the burst begins after synaptic activity.

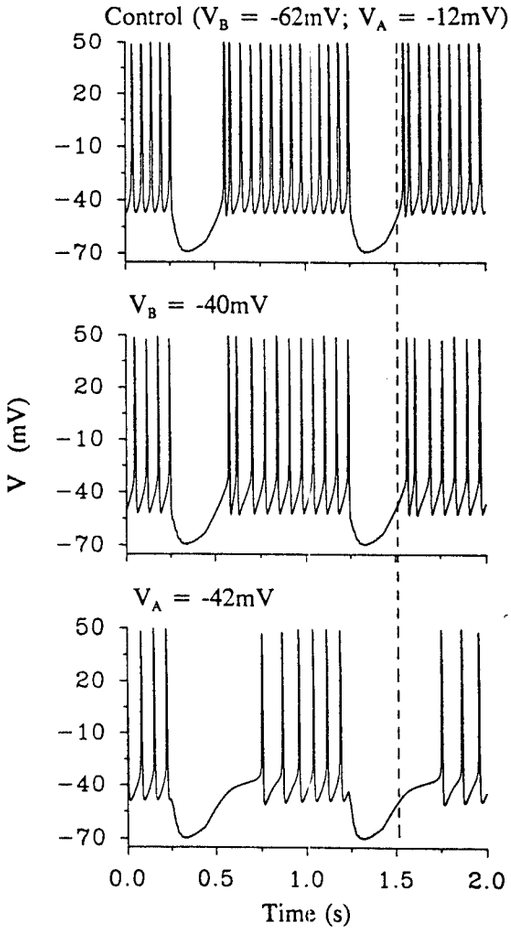

FIG. 11. Model cell's synaptic potentials: effect of i_A parameters. Standard model plus $\bar{g}_p$ set to ⅓ of its normal value to increase the firing frequency in a manner that mimics the activation of the pyloric cells by afferent fibers coming through the stn. Presynaptic activity is bursts of 10 IPSPs at 50 Hz every 1 s. *Top*: control (V_B = −62 mV; V_A = −12 mV). *Middle*: V_B = −40 mV; V_A = −12 mV. *Bottom*: V_B = −62 mV; V_A = −42 mV. Dashed line drawn for easier comparison among panels.

An unusual feature of the firing pattern seen in proctolin is that there is an increase in both the action-potential duration (which ordinarily one would expect to retard the next action potential) and the action-potential frequency. Although the increase in action-potential duration is relatively modest (10%, measured at −20 mV, Table 1), depending on the relationship of transmitter release to action-potential duration, this could have significant implications for the release of neurotransmitter by the LP neuron, especially because the intracellular Ca^{2+} concentration in proctolin shows a substantial increase in baseline values (Fig. 5).

Under normal physiological conditions the LP neuron receives phasic bursts of IPSPs that bring its membrane potential to values that are likely to activate i_h and deinactivate i_A and i_{Na}. Therefore we used simulated bursts of synaptic potentials to emulate conditions the LP cell is under within the network. These bring the model LP neuron into the voltage range in which i_h and i_A are likely to influence the activity of the LP neuron. Specifically, we simulated bursts that mimic those seen in the pyloric rhythm so that the time-dependent dynamics of i_h and i_A would be appropriately studied. Figure 10 demonstrates that i_h can strongly influence the waveform of synaptic potentials as well as the recovery from inhibition in the LP neuron. Thus phase relationships in the pyloric network can depend on the properties of i_h. It should be noted that the parameter changes we have used (i.e., doubling $\bar{g}_h$ and depolarizing by 15 mV the activation curve of i_h) are comparable with changes induced by serotonin in a different cell of the same ganglion (O. Kiehn and R. M. Harris-Warrick, unpublished observations).

i_A has been proposed to play a critical role in controlling the phase relationships of neurons in the pyloric rhythm (Hartline and Gassie 1979; Hartline et al. 1990). Indeed, Fig. 6 shows that i_A in the model neuron has the well-known attributes (Connor and Stevens 1971; Connor et al. 1977) of influencing the firing frequency and the latency to the first spike after inhibition. More interestingly, Fig. 11 demonstrates that shifting the voltage dependence of i_A activation and inactivation produces alterations in firing frequency and recovery from a simulated burst of IPSPs. This makes plausible the suggestion that differences in the properties of i_A in different classes of pyloric network neurons (Hartline et al. 1990; Tierney and Harris-Warrick 1990) may be important determinants of the phase relationships in the pyloric rhythm.

The effect of i_{Ca} on the model cell (Fig. 9) shows that it strongly affects the baseline membrane potential and firing frequency, both of which markedly decrease when i_{Ca} is blocked. The latter effect is not observed in the real LP cell, although the baseline potential does hyperpolarize somewhat. We do not have a clear explanation for this discrepancy, but it is conceivable that Cd^{2+} blocks some residual synaptic currents that, in control conditions (Fig. 9*B, top*), keep the cell from firing faster. In both the model and the real LP cell, however, blocking i_{Ca} does make action-potential duration longer, because of its indirect blocking effect on $i_{o(Ca)}$ (compare with Fig. 8). Blocking only one of the two components of i_{Ca} in the model does not mimic the Cd^{2+} effect either.

Models such as the one we have developed here allow us to do experiments that we are unable to do with biological preparations. Pharmacological agents that block completely one current without influencing others are rare. Moreover, in biological preparations it is very difficult to alter cleanly the maximal conductance of most currents. Although we were surprised by several of the results of our simulations, we are pleased that, once the model was constructed (Buchholtz et al. 1992), its responses to many of the perturbations presented in this paper mimicked well the results of biological experiments. Despite the inordinate complexity of a cell with so many dynamical variables, it is gratifying that the model neuron in most regards reinforced the intuitions we and others have obtained from voltage-clamp measurements.

The process of model construction forcefully reminds the physiologist of many unanswered problems. Specifically,

there is intrinsic variability in all biophysical measurements. For example, the values of maximal conductance for any current might differ from preparation to preparation. Indeed, the extent of this variability is often of the same magnitude as the perturbations of the model neuron investigated here. Fits to i_d in the LP cell of six different animals gave half-maximum potentials of activation (V_n) in the range of −14 to +5 mV, step width of activation (s_n) in the range of −22 to −11 mV, and maximum conductances ($\bar{g}_d$) in the range of 0.25–0.35 μS. This indicates that a large variability occurs in the different parameters that define this and other currents. However, biological neurons retain with extreme fidelity their characteristic electrical signatures. This may mean that most of the variability in physiological measurements is induced by the experimental procedure. Alternatively, neurons may have interesting compensatory feedback mechanisms that allow them to produce their essential patterns of activity despite modifications in some aspects of their currents. If so, this indicates the existence of important cellular processes not taken into account in this or similar models, as models are not often extremely robust with respect to parameter modifications. Our work thus highlights a fundamental puzzle of neuroscience: if the electrical activity of a neuron that confers on it its essential characteristics is so tied to the correct balance of many different conductances, how are these regulated so that the neuron retains its physiological identity throughout its lifetime, despite protein turnover and growth? Although mathematical models may not provide an answer to this question, they can help us understand the boundaries within which neurons must operate.

We thank Drs. L. F. Abbott, John Lisman, and Thomas Kepler for comments and criticisms of this work at different stages of its development. This paper benefited greatly from the comments of the *Journal of Neurophysiology* reviewers.

This work was supported by National Institutes of Health Grants NS-17813 and MH-46742 and by a fellowship from the Deutsche Forschungsgemeinschaft to F. Buchholtz.

Part of this work was submitted by J. Golowasch in partial fulfillment of the requirements for the PhD in Biophysics at Brandeis University.

Present address of J. Golowasch: Laboratoire de Neurobiologie, Ecole Normale Supérieure, 46 rue d'Ulm, 75005 Paris, France.

Address for reprint requests: E. Marder, Dept. of Biology, Brandeis University, Waltham, MA 02254-9110.

Received 31 May 1991; accepted in final form 4 September 1991.

REFERENCES

BUCHHOLTZ, F., GOLOWASCH, J., EPSTEIN, I. R., AND MARDER, E. Mathematical model of an identified stomatogastric ganglion neuron. *J. Neurophysiol.* 67: 332–340, 1992a.

CONNOR, J. A. AND STEVENS, C. F. Voltage clamp studies of a transient outward current in gastropod neural somata. *J. Physiol. Lond.* 213: 21–30, 1971.

CONNOR, J. A., WALTER, D., AND MCKOWN, R. Neural repetitive firing. Modifications of the Hodgkin-Huxley axon suggested by experimental results from crustacean axons. *Biophys. J.* 18: 81–102, 1977.

EISEN, J. S. AND MARDER, E. Mechanisms underlying pattern generation in lobster stomatogastric ganglion as determined by selective inactivation of identified neurons. III. Synaptic connections of electrically coupled pyloric neurons. *J. Neurophysiol.* 48: 1392–1415, 1982.

GETTING, P. A. Reconstruction of small neural networks. In: *Neuronal Modeling. From Synapses to Networks,* edited by C. Koch and I. Segev. Cambridge, MA: MIT Press, 1989, p. 171–194.

GOLOWASCH, J. *Characterization of a Stomatogastric Ganglion Neuron. A Biophysical and a Mathematical Description* (PhD dissertation). Waltham, MA: Brandeis Univ., 1990.

GOLOWASCH, J. AND MARDER, E. Ionic currents of the lateral pyloric neuron of the stomatogastric ganglion of the crab. *J. Neurophysiol.* 67: 318–331, 1992a.

GOLOWASCH J. AND MARDER E. Proctolin activates an inward current whose voltage dependence is modified by extracellular Ca^{2+} *J. Neurosci.* In press, 1992b.

GRAUBARD, K., RAPER, J. A., AND HARTLINE, D. K. Graded synaptic transmission between identified spiking neurons. *J. Neurophysiol.* 50: 508–521, 1983.

HARTLINE, D. K. AND GASSIE, D. V. Pattern generation in the lobster (*Panulirus*) stomatogastric ganglion. I. Pyloric neuron kinetics and synaptic interactions. *Biol. Cybern.* 33: 209–222, 1979.

HARTLINE, D. K., GASSIE, D. V., TOMIYASU, B. A., AND JONES, B. R. Ionic current fingerprints in lobster stomatogastric neurons. *Soc. Neurosci. Abstr.* 16: 1131, 1990.

HODGKIN, A. L. AND HUXLEY, A. F. A quantitative description of membrane current and its application to conduction and excitation in nerve. *J. Physiol. Lond.* 117: 500–544, 1952.

HOOPER, S. L. AND MARDER, E. Modulation of the lobster pyloric rhythm by the peptide proctolin. *J. Neurosci.* 7: 2097–2112, 1987.

MARDER, E. Mechanisms underlying neurotransmitter modulation of a neuronal circuit. *Trends Neurosci.* 7: 48–53, 1984.

MARDER, E., HOOPER, S. L., AND SIWICKI, K. K. Modulatory action and distribution of the neuropeptide proctolin in the crustacean stomatogastric nervous system. *J. Comp. Neurol.* 243: 454–467, 1986.

NUSBAUM, M. P. AND MARDER, E. A modulatory proctolin-containing neuron (MPN). I. Identification and characterization. *J. Neurosci.* 9: 1591–1599, 1989a.

NUSBAUM, M. P. AND MARDER, E. A modulatory proctolin-containing neuron (MPN). II. State-dependent modulation of rhythmic motor activity. *J. Neurosci.* 9: 1600–1607, 1989b.

TIERNEY, A. J. AND HARRIS-WARRICK, R. M. 4-Aminopyridine alters cycle frequency and phase relationships among pyloric neurons in the lobster stomatogastric ganglion. *Soc. Neurosci. Abstr.* 16: 1296, 1990.